



Size-resolved aerosol and cloud condensation nuclei (CCN) properties in the remote marine South China Sea, Part 1: Observations and source classification

Samuel A. Atwood¹, Jeffrey S. Reid², Sonia M. Kreidenweis¹, Donald R. Blake³, Haflidi H. Jonsson⁴,
5 Nofel D. Lagrosas⁵, Peng Lynch⁶, Elizabeth A. Reid², Walter R. Sessions^{6,7}, James B. Simpas⁵

¹Department of Atmospheric Science, Colorado State University, Ft. Collins, CO

²Marine Meteorology Division, Naval Research Laboratory, Monterey, CA

³Department of Chemistry, University of California, Irvine, CA

⁴Department of Meteorology, Naval Postgraduate School, Monterey, CA

10 ⁵Manila Observatory, Manila, Philippines

⁶CSC Inc. at Naval Research Laboratory, Monterey, CA

⁷Space Sciences Engineering Center, University of Wisconsin, Madison, WI

Correspondence to: Jeffrey S. Reid (jeffrey.reid@nrlmry.navy.mil)

Abstract. Ship-based measurements of aerosol and cloud condensation nuclei (CCN) properties are presented for two weeks
15 of observations in remote marine regions of the South China Sea/East Sea during the Southwestern Monsoon (SWM) season. Smoke from extensive biomass burning throughout the Maritime Continent advected into this region during the SWM, where it was mixed with anthropogenic continental pollution and emissions from heavy shipping activities. Eight aerosol types were identified using a K-Means cluster analysis with data from a size-resolved CCN characterization system, additional onboard aerosol and meteorological measurements, and satellite and model products for the region. A typical
20 bimodal marine boundary layer background aerosol population was identified that was observed mixing with accumulation mode aerosol from other sources, primarily smoke from fires in Borneo and Sumatra. Hygroscopicity was assessed using the κ parameter and was found to average 0.40 for samples dominated by aged, accumulation mode smoke; 0.65 for accumulation mode marine aerosol; 0.60 in an anthropogenic aerosol plume; and 0.22 during a short period that was characterized by elevated levels of volatile organic compounds not associated with biomass burning impacts. As a special
25 subset of the background marine aerosol, clean air masses substantially scrubbed of particles were observed following heavy precipitation or the passage of squall lines, with changes in observed aerosol properties occurring on the order of minutes. Average CN number concentrations, size distributions, and κ values are reported for each population type, along with CCN number concentrations for particles that activated at supersaturations between 0.14% and 0.85%.

30 **Keywords.** Remote Marine Aerosol, Cloud Condensation Nuclei, Biomass Burning, South China Sea, Source Apportionment, K-Means, Mixing State



1 Introduction

Assessment of regional aerosol properties in the Southeast Asian Maritime Continent (MC) and South China Sea/East Sea (SCS) regions has proven difficult. Extensive cloud cover confounds remote sensing and leads to a clear sky bias in observations (Feng and Christopher, 2013; Reid et al., 2013). Aerosol monitoring has largely been confined to urban centers that are often dominated by local emissions, while in-situ sampling in remote areas has been limited in duration and scope (Irwin et al., 2011; Robinson et al., 2011; Lin et al., 2014; Reid et al., 2015). Airborne measurements have provided some representation of aerosol over wider regions and at various levels (Hewitt et al., 2010; Robinson et al., 2012), but additional questions regarding the impact of various sources on surface aerosol concentrations and the representativeness of results across larger time scales remain. Thus, over these remote ocean regions the aerosol optical and physical properties, their variability in time and space, and the processes controlling aerosol lifecycle have not been well constrained. This uncertainty in the aerosol environment itself comes in addition to uncertainty about its impacts on meteorological processes. Aerosol concentration has been found to relate to cloud development, cloud microphysics, and precipitation formation in the region (Yuan et al., 2011; Wang et al., 2013), while smoke may affect cloud droplet size distributions and the onset of precipitation, similar to processes observed in other tropical regions impacted by biomass burning (Rosenfeld, 1999; Andreae et al., 2004). Improved knowledge of the aerosol environment and aerosol-cloud-climate relationships in the Southeast Asian region has therefore been identified as important regionally, and in regards to links with global climate and large-scale aerosol budgets (Reid et al., 2013).

During the May through October Southwestern Monsoon (SWM) season, burning throughout the MC typically reaches its greatest extent between August and early October as precipitation associated with the ITCZ shifts north into Indochina (Reid et al., 2012). The resulting heavy smoke mixes with urban, industrial, marine, and shipping emissions in an exceedingly complex aerosol mixture (Balasubramanian et al., 2003; Atwood et al., 2013; Reid et al., 2013). During this period, aerosol particles from surface sources are generally advected by low level mean winds throughout the SCS, where they are scavenged by precipitation or eventually removed in the monsoonal trough east of the Philippines (Reid et al., 2012, 2015; Wang et al., 2013; Xian et al., 2013). As a result, the region of the SCS and Sulu Sea to the north and east of Borneo has been predicted to be a receptor for much of these biomass burning and pollution emissions from the greater MC during periods when air masses enter more convective phases of the SWM (Reid et al., 2012; Xian et al., 2013).

Two research cruises in this area were conducted during the 2011 and 2012 SWM to take advantage of these conditions and perform in-situ aerosol and meteorological measurements in the remote marine boundary layer (MBL) in the SCS and Sulu Sea (Reid et al., 2015, 2016). In this paper, we present observations of aerosol and CCN characteristics during the second cruise, and their relationship to aerosol source type, air mass, and meteorological phenomena. These measurements represent the first in situ observations of size-resolved CCN properties, and fill a gap in knowledge needed to assess aerosol-cloud-precipitation relationships in the in the data poor remote marine SCS region.



2 Methods and Cruise Description

The SCS research cruises occurred during the month of September in both 2011 and 2012, and took place aboard the 35m, 186 ton *M/Y Vasco*, operated out of Manila by Cosmix Underwater Research Ltd. A thorough description of the vessel and instrumentation for the 2011 and 2012 cruises can be found in Reid et al. (2015) and Reid et al. (2016), respectively. Here we are concerned with the 2012 cruise, which departed Manila on 4 September from Navotas, Manila Bay, and returned on 29 September. The sampling strategy for these cruises involved moving between various anchorages in the SCS and Sulu Sea around the Palawan Archipelago. Sampling occurred throughout the cruise, but aerosol measurements were shut down during periods when representative sampling could not be achieved (i.e., incompatible mean winds and ship orientation). Remaining periods of self-sampling of ship emissions were identified by anomalous size distributions and high particle number concentrations, and were removed from the data set before analysis. The size-resolved CCN system (Petters et al., 2009) that provided the bulk of the measurements reported here had a computer failure that, once fixed, limited reliable measurements to primarily the last two weeks of the cruise, hence we focus here on data from 14-26 September 2012. This period included several transits along the east side of Palawan Island, stationary measurements at an anchorage between Palawan and Borneo (7.86N, 116.94E), and two anchorages at Tubbataha Reef in the middle of the Sulu Sea (8.80N, 119.26E).

The NOAA Hybrid Single Particle Lagrangian Integrated Trajectory (HYSPPLIT) Version 4.9 model (Draxler et al., 1999; Draxler and Hess, 1997, 1998) was used to generate daily 72-hour backtrajectories from the *Vasco* location with arrival heights of 500m to indicate likely boundary layer transport patterns. The GDAS1, 1° x 1° HYSPPLIT meteorological dataset was used to drive the model.

2.1 Aerosol Measurements

A DMT PCASP X2 configured in an aviation pod with heated inlet was mounted at the *Vasco* top mast to provide optical measurements of dry particle size distributions between approximately 125 nm and 3 µm. Additional aerosol instrumentation was located in a forward locker, below and slightly behind the aerosol inlet. Sampled air was fed to the locker via a 3 cm diameter, 4 m long inlet located next to the PCASP. Although the inlet was not aspirated, several high flow rate nephelometers sampling from the inlet ensured low residence time in the sample line. Further details and additional instrumentation are discussed in Reid et al. (2016). A size resolved CCN system sampled air from the inlet just inside the instrument locker with an approximately 2 m, 0.635 cm diameter copper tube. A URG cyclone with an approximate 1 µm 50% size cut was used to remove the largest particles from this CCN sampling line, including coarse mode sea-salt, to minimize wear and corrosion on downstream components. The sample was then dried using a Permapure poly-tube Nafion dryer with low pressure sheath air.

Approximately 1.1 liters per minute (lpm) were drawn through the size resolved CCN system, which was comprised of an x-ray neutralizer (TSI Model 3087) and a TSI 3080 Electrostatic Classifier with a long DMA column (TSI Model 3081) for



quasi-mono-disperse particle sizing, preceded by a 0.071 cm orifice (0.69 μm 50% cutpoint diameter) impactor. The DMA was operated with a sheath flow rate of 5 lpm (liters per minute) and sample flow rate of 1.1 lpm. The sample flow was then split between a TSI 3782 Water Condensation Particle Counter (CPC) with a flow rate of 0.6 lpm, and a DMT Cloud Condensation Nuclei Counter (CCNc) with a flow rate of 0.5 lpm. Flow rates used to calculate number concentrations were calibrated using a Gilibrator (Models 800285 & 800286) system.

The size-resolved CCN system measured CN and CCN (activated particles at CCNc set-point supersaturation) concentrations in each of 30 quasi-mono-disperse size bins between 17 nm and 500 nm. The CCNc was operated at five temperature gradient settings and calibrated using ammonium sulfate (following the methods described by Petters et al. (2009)) to measure the corresponding maximum environmental supersaturation within the CCNc column. Calibrated supersaturation set-points and their respective standard deviations were $0.14\% \pm 0.01$, $0.38\% \pm 0.01$, $0.52\% \pm 0.01$, $0.71\% \pm 0.02$, and $0.85\% \pm 0.03$. The scan of all 30 size bins at each supersaturation took approximately 15 minutes, while a complete measurement over all 5 supersaturation settings took approximately two hours due to pauses between settings while column temperatures stabilized. The measured CN and CCN particle counts were inverted using the methodology of Petters et al. (2009). The inversion yielded the dry ambient aerosol size distribution over the measured range ($dN/d\log_{10}D_p$ for $17 \leq D_p \leq 500$ nm) and CCN activation spectra at each supersaturation, expressed as the fraction of total particles (CN/CCN) of diameter D_p that formed droplets. Each activated fraction spectrum was fit using a three parameter fit similar to the approach of Rose et al. (2010). The diameter at which 50% of particles in the fit had activated (D_{50}) was used to calculate the associated hygroscopicity parameter, κ (Petters and Kreidenweis, 2007). As the SCS environment tended to have relatively few particles smaller than 50 nm, only the measurements at the 0.14% and 0.38% supersaturation settings had complete activation curves that spanned the measured particle diameter range. For the higher supersaturation settings, the D_{50} diameter tended to occur at small diameters with low CN and CCN concentrations, thereby increasing uncertainty in the associated κ values. As a result, κ values were only reported for the 0.14% and 0.38% supersaturation settings.

2.2 Ancillary Measurements and Products

Additional measurements of aerosol composition were used to validate identified source types impacting the measurements throughout the cruise. A series of $\text{PM}_{2.5}$ filters were collected by 5 lpm Minivol Tactical Air Samplers that were analyzed for elemental concentrations by gravimetric, XRF, and ion chromatography methods, and organic and black carbon concentrations by the thermal-optical methods. Trace gas concentrations were measured intermittently throughout the cruise by whole-air gas samples for gas chromatography analysis, as discussed further in Reid et al. (2016).

A suite of weather monitoring instruments was located on a 3m bow mast to provide coincident meteorological measurements throughout the study. From this suite, wind speed and wind direction measurements from a Campbell sonic anemometer were used to identify gust front passage. An OTT Parsivel disdrometer was utilized to measure precipitation, from which only the rain rate measurements were used in this analysis.



Several remote sensing and model products were used to characterize the wider SCS atmospheric environment and to identify potential aerosol sources. MODIS visible and IR products were used to identify convection and squall line propagation across the SCS. MODIS active fire hotspot analysis and the FLAMBE smoke flux product from Terra and Aqua were used to identify the locations and times during which fires were burning in the MC (Giglio et al., 2003; Reid et al., 2009; Hyer et al., 2013). Simulations from the Navy NOGAPS model were used to represent surface and 700 hPa winds and thereby estimate likely aerosol transport pathways throughout the study (Hogan and Rosmond, 1991). Finally, the Navy Aerosol Analysis and Prediction System (NAAPS) was used to predict smoke and sulfate aerosol mass concentrations at the surface along the *Vasco* ship track (Lynch et al., 2016).

2.3 Aerosol Population Type Classification

The $dN/d\log_{10}D_p$ dry particle size distributions obtained every 15 minutes from the CCN system were first normalized by the particle number concentration summed over all bins. Each of these normalized size distributions was then parameterized by fitting a lognormal mixture distribution using an algorithm based on Hussein et al. (2005). This algorithm fit each distribution to one, two, or three lognormal modes, each described by three lognormal distribution parameters (median diameter, geometric standard deviation, and fractional number concentration)—which identified a best-fit using two modes for 690 of 731 data points in this dataset. In order to have a common point of comparison for classification purposes a two mode best-fit was used, yielding a parameterized Aitken and accumulation mode for each 15-minute data point—data points for which the fitting algorithm selected an additional third mode are noted in the clustering results in Sect. 4.

These normalized size distribution parameters were then combined with hygroscopicity and total number concentration measurements to serve as input variables for an unsupervised cluster analysis. A hierarchical cluster analysis was first conducted using the *cluster.AgglomerativeClustering* class of the Python scikit-learn package (Pedregosa et al., 2011) using the Ward linkage to help ascertain the number of clusters that can be found in the dataset. Each step in this process involved merging two data points or clusters into a new cluster based on those points with the closest distance between normalized input measurements (Karl Pearson distance function). A dendrogram and associated measure of the distance between merged clusters for each subsequent clustering step was used to identify potential numbers of clusters appropriate for the dataset. The distance between merged clusters increases at steps that merge substantially different clusters (Wilks, 2011)—in this case indicating 5, 8, 9, and 12 clusters as potentially appropriate for this data set.

A nonhierarchical K-Means cluster analysis was then conducted for each of these four potential cluster numbers using the scikit-learn *cluster.KMeans* class to refine the cluster members. The appropriate number of clusters to classify the dataset according to was identified based on the K-Means result with the least number of clusters that maintained physically distinct and temporally consistent aerosol populations for the associated clusters. In particular, as the timestamp of a data point was not included in the cluster analysis, clusters with smaller numbers of data points were considered distinct if they all occurred during a narrow time frame that could be associated with a transient atmospheric phenomenon. The time frames of all clusters were then compared against other aerosol and meteorological observations to ensure they were physically



meaningful. The result was a set of eight identified aerosol population types with associated time periods corresponding to the 15 minute CCN system data points. Finally, size distribution and hygroscopicity measurements were averaged for all time periods associated with each population type.

3 Results

5 3.1 Overview of Study

The daily positions of the *Vasco* during the two weeks in September 2012 that comprise this study are shown in Figure 1a, together with HYSPLIT 72-hour backtrajectories initiated within the MBL. The daily fire hot spots are also indicated in this figure. Average NOGAPS surface winds in the boundary layer were from the southwest, often advecting air parcels from near Borneo, while lower free tropospheric winds, such as those at 700 hPa, were more westerly due to the generally veering structure of the lower atmosphere in the SCS (Reid et al., 2016). Fires detected by MODIS occurred throughout much of Borneo and Southern Sumatra during the study, with surface-level trajectories near the start and near the end of the study period passing close to active fires, whereas those during the middle period remained primarily over open ocean. Results from the NAAPS model, along with limited satellite AOD measurements not obscured by clouds during this period, confirmed this general smoke transport pathway. Accumulation mode aerosol mass concentrations (Figure 1b) were derived from the PCASP measurements using a density of $1.4 \mu\text{g m}^{-3}$ (Levin et al., 2010), assumed to be representative of a combination of smoldering peat and agricultural fire emissions typical in the MC (Reid et al., 2012). Mass concentrations were highest early and late in the measurement period, in general agreement with the backtrajectories passing over terrestrial sources and active fires and with NAAPS modeled surface aerosol smoke and sulfate concentrations (Figure 1b). Air parcels advecting into the SCS and Sulu Sea during this period that originated from areas further to the north and west were cleaner than those from other sectors, due to fewer emission sources and more precipitation along the trajectories. Changes in the observed particle concentrations also occurred on timescales shorter than these weekly large-scale variations, as shown in the aerosol observation timelines in Figures 2a-c. Many of these higher-frequency fluctuations were associated with squall line passages and heavy local precipitation, as discussed further in the following section. The timeline of $dN/d\log D_p$ size distributions, as measured by the CCN system and shown in Figure 2a, indicates that most of the particle number concentration fell within the 17-500 nm measurement range, except possibly during the highest-concentration periods. A more extensive comparison of model and satellite measurement in situ observations is discussed in Reid et al. (2016).

3.2 Analysis of Daily Observations

At the start of the measurement period on 14 Sept., the *Vasco* was in transit south from Puerto Princessa, Philippines, in the middle of the island towards Balabac Island at the southern edge of Palawan Archipelago. HYSPLIT 500 m backtrajectories on this day identified MBL transport from the southwest over burning regions in Borneo (Figure 1a). As shown in Figure 2, at the start of the campaign, high number concentrations of accumulation mode particles (1500 to 4000 cm^{-3}) with generally



mono-modal size distributions were observed (best fit lognormal median diameters around 200 nm), consistent with expectations for aged smoke. Elevated concentrations of potassium, carbon monoxide, and benzene during this period (Reid et al., 2016, and Figure 2c) all reinforce the classification of this aerosol as smoke (Yokelson et al., 2008; Akagi et al., 2011; Reid et al., 2015). This initial smoke impacted period was followed by a drop in particle number concentrations after 12Z on 5 14 Sept. as a squall line passed over the *Vasco* and left a clean air mass scrubbed of many of the particles. Total particle number concentrations were among the lowest values observed during the cruise, with fewer than 200 cm^{-3} measured in the 17-500 nm range. Particle number concentrations did not recover for approximately 10 hours, at which point the aerosol size spectra and concentrations resembled those measured in the air mass before the gust front passage.

The *Vasco* remained at the same anchorage at Balabac Island on the southern tip of the Palawan Archipelago until 19 Sept. 10 Beginning at about 5Z on 17 Sept., particle number concentrations dropped, but not as low nor as rapidly as during the post-squall-line event. A distinct bimodal size distribution was observed that coincided with the onset of precipitation observed at the boat (Figure 2d). Satellite visible and IR imagery (not shown) indicated that no long lived squall line was associated with this 17 Sept. precipitation event. Beginning around 18Z on 17 Sept. number concentrations began to increase and a third mode of particles with diameters between 20 and 30 nm was observed (Figure 2a). This mode slowly mixed into the Aitken 15 mode as more typical bimodal distributions resumed by the middle of 18 Sept. A filter during this period showed very low potassium concentrations, with benzene among the lowest values measured during the study, indicating that biomass burning was not the likely source for this event. In addition, at the start of this period several volatile organic compound species (VOCs) were elevated as compared to periods before and after the event. Anthropogenic, shipping, and marine and terrestrial biogenic emissions are known sources of such compounds; isoprene, a common biogenic VOC, was not observed during this 20 event, and a brief period of elevated dimethyl sulfide, associated with marine emissions from phytoplankton, was observed shortly before—but not during—this event (Reid et al., 2016).

The data gap on 19 Sept occurred during the return transit to Puerto Princessa, as the trailing winds caused self-sampling of boat emissions. However, westerly winds allowed for sampling once the *Vasco* turned to head into port, and measurements were continued for several hours to characterize emissions from the port and the city with a population of over 200,000. 25 Number concentrations in port were considerably higher than in the remote marine locations of the SCS, with total number concentrations between 4000 and $10,000\text{ cm}^{-3}$ in the 17-500 nm size range. Ultrafine particles ($D_p < 100\text{ nm}$) dominated number concentrations during this period, although large number concentrations of accumulation mode particles with diameters between 100 and 300 nm were also observed.

The *Vasco* departed the port and sailed on an east-southeasterly course late on 20 Sept., during a period when both NOGAPS 30 and the onboard weather tower indicated generally westerly low-level winds. This wind direction allowed for measurements of the Puerto Princessa urban plume as it was transported out over the Sulu Sea. Particle number concentrations between roughly 750 and 2000 cm^{-3} were measured during this period, with size spectra showing a mode with 80-90 nm median diameters. This modal median diameter was unique during the cruise; modal median diameters in the 40-70 nm or 150-225



nm ranges were more commonly observed. As the *Vasco* moved further to the southeast and out of the city plume, the size distribution measurements began to more closely resemble the previously seen bimodal background marine conditions.

The *Vasco* arrived at the remote Tubbataha reef in the middle of the Sulu Sea on 21 Sept and remained there through the end of the measurement period on 27 Sept. Throughout this time, the inflow arm of a nearby tropical cyclone spawned large amounts of intermittent convection and cloud cover over much of the SCS and Borneo. Measured number concentrations and size distributions showed considerable variation during this period as transport of smoke from Borneo was intermixed with cleaner periods associated with precipitation events. A final larger smoke event occurred on 25 and 26 Sept shortly before the end of the measurement period. This event was similar to the early smoke dominated period with largely mono-modal size distributions and total particle number concentrations above 2000 cm^{-3} , and was followed by mixing and a return to background marine conditions.

3.3 Aerosol Population Type Classification and Properties

The parameter values input to the cluster analysis are shown for each data point and variable in Figure 3, and colored by cluster number for the results of the eight-cluster K-Means analysis. Normalized size distributions for each of these eight aerosol populations are shown in Figure 4; the average CN and CCN number concentrations and hygroscopicities are given in Table 1. Equivalent normalized volume distributions are shown in Supplementary Figure S1. The cluster number associated with each measurement is similarly shown as the background color in Figure 2 and marker color in Figure 5. A name identifying the likely source of each population type was then assigned as follows, on the basis of the previously identified meteorological and other factors discussed in Sect. 3.2. Clusters 1-4 were the most commonly found (representing 85% of the total observations, Table 1), while clusters 5-8 represented special cases, generally of short duration, that could be identified with specific locations or sampling conditions.

1. Background Marine: This population was similar to the background marine aerosol reported in many prior studies (e.g. Hoppel et al., 1994; O'Dowd et al., 1997; Spracklen et al., 2007; Good et al., 2010), and consisted of a bimodal size distribution with a Hoppel minimum (Hoppel et al., 1986) near 90 nm due to cloud or fog processing. The inner quartile range (IQR: middle 50% of observations between the 25%–75% percentiles) of number concentrations ranged from 382 to 623 cm^{-3} , with on average 42% of the total number concentration residing in the accumulation mode as specified by the bimodal fit.
2. Precipitation: This distribution was found in scrubbed air masses where accumulation mode particles had been preferentially removed. While the number concentrations of large-mode particles were lower than those in the background marine periods, the number concentrations of smaller particles, particularly those below 40-50 nm, were comparable to the clean marine type. Identified periods were nearly always associated with precipitation at or near the *Vasco* (Figure 2d) and extended periods of this type occurred in the wake of the squall lines, though not all instances of nearby precipitation lead to this type. Number concentrations tended to be lower than the clean marine type with an IQR from 227 to 441 cm^{-3} .



3. Smoke: In this aerosol type, particles were largely concentrated in a single accumulation mode with a tail of smaller particles. This type was associated with the highest total particle number and submicron mass concentrations observed during the cruise, with the exception of measurements taken in the urban plume of Puerto Princessa. The standard deviations in the normalized size distribution parameters for this population in Figure 4 were small, even while number concentration varied widely (IQR 1802 to 2780 cm⁻³; 81% accumulation modal fraction). While smoke is considered the dominant aerosol source during these periods, anthropogenic pollution may still contribute.
4. Mixed Marine: This population was characterized as periods when the background marine type was mixing with other sources of aerosol. Most of the data points associated with this type had transport pathways and biomass burning sources similar to those for the smoke population type, but with concentrations, size distribution parameters, and hygroscopicities between those of the clean marine and smoke types (IQR 782 to 1160 cm⁻³; 68% accumulation modal fraction), indicating there was insufficient smoke for it to dominate the properties of the marine background. Air masses influenced by anthropogenic pollution may occur in this cluster as well, but without sufficiently different impacts on aerosol parameters to justify a distinct cluster.
5. Organic Event: An approximately four hour period starting at 1Z on 23 Sept had measured particle concentrations between 200 and 325 cm⁻³, but with significantly ($p < 0.001$) larger median diameters than either the precipitation or background marine types (Figure 3). Both Aitken and accumulation mode particles had among the lowest hygroscopicities measured during the cruise, with κ values around 0.2. During this event measured concentrations of numerous VOCs were much higher than in gas canisters collected approximately 6 hours before and after it with no associated increase in carbon monoxide (Reid et al., 2016; Figure 2c). The particles had lower hygroscopicities and larger sizes than the background marine particles which were observed just before this event. Robinson et al. (2012) found occasional organic aerosol above the boundary layer they attributed to biogenic Secondary Organic Aerosol (SOA) formation during an airborne campaign in the outflow regions of Borneo. Such a source might create aerosol similar to this type, although we lack the ancillary data needed to establish this.
6. Ultrafine Event: A period of elevated VOC measurements as discussed in Sect. 3.2, which coincided with the largest concentrations of particles below about 30 nm during the study. A tri-modal best-fit was indicated by the Hussein, et al. (2005) algorithm for a number of these data points (Figure 2a). The period had an overall IQR of 482 to 661 cm⁻³, with generally higher ultrafine number concentrations than other periods with similar total concentrations. The accumulation mode was similar in both size and hygroscopicity to the accumulation mode of the background marine type, while the smaller Aitken mode showed larger modal fractions and overall number concentrations than the clean marine measurements. While not enough information is available to verify the nature of differences between ultrafine particles in these types, the results are consistent with an influx of smaller particles and VOCs into a background marine air mass, and were sufficiently distinct to be identified as a coherent period by the unsupervised K-Means analysis.



7. Transit: This type was assigned to the cluster that identified measurements taken during the transit from the port to the east of Puerto Princessa, when westerly winds advected anthropogenic pollution over the Sulu Sea. Size distributions were dominated by an Aitken mode with a number median diameter around 80-90 nm, mixed with an accumulation mode with a smaller modal fraction than other types. The size distribution measurements were consistent with an urban plume diluting via mixing with background marine type aerosol, and had an IQR of 738 to 1029 cm^{-3} .
8. Port: This type was assigned to the measurements taken during the short period in the port of Puerto Princessa. Local anthropogenic emissions were dominant during this period, with number concentrations between 4000 and 10,000 cm^{-3} . The majority of particles were in the ultrafine size range ($D_p < 100$ nm). This type is considered separate from the other types as it was not measured in a remote marine area away from the immediate influence of a nearby terrestrial source.

Finally, throughout the study coarse mode particles with diameters larger than about 800 nm were consistently observed in the PCASP volume distributions (Figure 2b). Concentrations of particles in this size range increased with increasing wind speed (Figure 5), consistent with generation of sea spray aerosol due to bubble breaking and wave action (O'Dowd and Leeuw, 2007), and with less of a relationship to submicron aerosol population type. Particles in this size range are not measured or accounted for in our measurements (CCN system range: 17-500 nm). While the number of particles in this size range is small compared to typical CCN concentrations (Figures 2e, f), in the cleanest conditions we measured they represented non-trivial fractions of CCN active at 0.14% and 0.38% supersaturations. The large diameter of these particles makes them likely to activate at very low supersaturations, and they are present in more than sufficient number concentration to impact the microphysical structure and processes in stratocumulus clouds by serving as "giant CCN" (Feingold et al., 1999).

3.4 Aerosol Hygroscopicity

The hygroscopicity parameter, κ , can be used to quantify the expected role of particle composition on water uptake and activation to cloud droplets (Petters and Kreidenweis, 2007). Anthropogenic pollution from urban areas often includes highly hygroscopic species such as ammonium sulfate ($\kappa = 0.61$) and ammonium nitrate ($\kappa = 0.67$), although non- or weakly-hygroscopic species such as black carbon and nonpolar organic species are also common aerosol components. Fresh sea spray particles, dominated by sodium chloride ($\kappa = 1.28$), are expected to have the highest κ values (Good et al., 2010), although co-emitted organic species and replacement of chlorine by uptake of acidic gases can potentially reduce κ . Aged biomass burning aerosol or organic dominated particle populations have generally been found to have κ values below 0.2, while black carbon ($\kappa \approx 0$) has very low hygroscopicity (Andreae and Rosenfeld, 2008; Petters et al., 2009; Engelhart et al., 2012). Similar size-resolved hygroscopicity measurements were performed in a remote rainforest location in Borneo by Irwin et al. (2011) during a time period with little to no biomass burning. They reported κ values between 0.05 and 0.37 for this terrestrial, biogenically dominated MC environment.



The range of κ values measured for the particles active at supersaturations of 0.14% and 0.38% was typically between about 0.3 and 0.8, although the full range was between 0.2 and 1.1 (Figures 2e, f). Average hygroscopicities and standard deviations for each population type at the 0.14% and 0.38% supersaturations are presented in Table 1, along with the average CN and CCN concentrations across all supersaturation settings. It is important to note that particle sizes (D_{50} : characteristic particle diameter at which 50% of particles in the CCNc have activated) corresponding to these measurements are in the range of 45 – 150 nm; our measurements did not characterize the hygroscopicities of either the very small particles ($D_{50} < 45$ nm) nor the particles with diameters above ~150 nm.

The 0.14% supersaturation scans have D_{50} diameters that span approximately 96 to 150 nm for κ values between the approximate observed range of 0.8 and 0.2, respectively. Hygroscopicity measurements at this lowest supersaturation are therefore more sensitive to particles in the larger accumulation mode—hence our segregation of a subset of observations of κ into accumulation and Aitken parameters for clustering purposes. The averaged properties in Table 1 indicated that such accumulation mode particles had lower average hygroscopicities ($\kappa = 0.40$) in the smoke population type as compared to the precipitation, background marine, ultrafine event, and transit populations ($\kappa = 0.54, 0.65, 0.65, 0.58$, respectively), while the mixed marine population ($\kappa = 0.48$) resided between these. High concentrations of both SO_2 and sulfate aerosol from numerous sources have been observed in the MC (Robinson et al., 2011; Reid et al., 2013). During this study, multi-day filter samples showed average sulfate concentrations between approximately 0.8 and 3 $\mu\text{g}/\text{m}^3$ at the *Vasco*, potentially increasing during periods of smoke impacts due to burning of sulfur rich peat in the region (Reid et al., 2016). The potential peat source or mixing with other sources of sulfate may explain the higher than typical κ values for aged biomass burning aerosol.

The hygroscopicities derived from measurements at the 0.38% supersaturation set-point had different trends. At the 0.38% supersaturation setting, activation occurs for particles sized between roughly 45 and 80 nm for particles in the observed 1.1 to 0.2 κ range, respectively, and thus measurements at this supersaturation were more closely identified with Aitken mode particles. During smoke impacted periods, the Aitken mode particles had κ values of 0.56 as compared with the 0.40 value observed in the accumulation mode. The aged, primary emissions from biomass burning are likely to be confined to particles larger than ~100 nm (Figure 4), and it is therefore possible that the Aitken mode particles in this population were largely derived from background sources rather than from biomass burning, leading to the higher observed κ values.

Interestingly, the opposite situation occurred in the background marine and precipitation aerosol populations, where the Aitken mode was less hygroscopic than the accumulation mode (clean marine: $\kappa = 0.46$ and $\kappa = 0.65$, respectively; precipitation: $\kappa = 0.34$ and $\kappa = 0.54$, respectively). Decreasing hygroscopicity with size is consistent with an increasing organic fraction at smaller particle sizes in marine aerosol, as has been observed both in field data and in the laboratory (Cavalli et al., 2004; O'Dowd et al., 2004; Facchini et al., 2008; Prather et al., 2013). These observations are also consistent with precipitation removal of some of the background sulfate aerosol, leading to lower hygroscopicities in cleaner aerosol populations due to marine organic aerosol becoming more dominant.



Finally, the organic event type had the lowest values ($\kappa \approx 0.2$) in both modes from the entire study. A gas canister grab sample during this period showed elevated levels of a number of organic compounds (Reid et al., 2016; Figure 2c), while the size distributions were similar to those of the background marine population type, but with slightly larger diameters (Figures 3 & 4). These results are consistent with particles dominated by organics across all sizes, perhaps due to growth of a background population by condensation of organics.

4 Discussion

Based on this classification of the SCS remote marine boundary layer aerosol environment, a conceptual picture emerges as to the nature and sources of particles encountered during the *Vasco* 2012 cruise. A bimodal marine aerosol background was present with number concentrations usually between about 300 and 700 cm^{-3} and a Hoppel minimum around 90 nm. Primary emissions via sea spray supply submicron particles consisting of a mixture of sea salt and organic components, with emitted particle diameters as small as 20 nm (Clarke et al., 2006; O'Dowd and Leeuw, 2007; Prather et al., 2013), but even in remote marine environments, transported anthropogenic and combustion aerosol may still be an important or even dominant source of small particles (Shank et al., 2012). The background marine population identified in this study is thus a background state across the remote SCS that is likely comprised of a mixture of primary marine emissions along with particles derived from anthropogenic and biomass burning sources throughout the region. Departures from the typical range of background marine characteristics and number concentrations occurred under large influxes of aerosol from other sources, such as smoke from biomass burning regions, anthropogenic pollution from population centers or shipping, or when convection and precipitation removed much of the ambient particulate matter and created relatively clean air masses.

During the SWM when large amounts of biomass burning aerosol were being advected into the SCS, a population of aged, accumulation mode smoke particles was periodically injected into the MBL where it mixed with existing particles. When total particle concentrations were above roughly 1500 cm^{-3} , the smoke particles dominated the background clean marine particles and had characteristic size distribution parameters and hygroscopicities that remained roughly constant regardless of the concentrations of biomass burning particles. In situations when smoke concentrations were insufficient to dominate the background marine aerosol population, a mixture of smoke and clean marine population types was present, with size distribution and hygroscopicity parameters in between the two types.

Precipitation removes particles that have been advected into the region, returning the environment near the surface to its clean marine background state. However, when extensive precipitation occurred, accumulation mode particles were removed by wet deposition to a greater extent than Aitken mode particles, leading to lower overall surface number concentrations that were dominated by smaller particles. Based on the two *Vasco* cruises, the cleanest periods were encountered in cold pools following the passage of squall lines with number concentrations as low as 100 to 150 cm^{-3} . During these periods, increased number concentrations of coarse mode aerosol were regularly observed (Figure 5; $\text{CN}_{>800}$: $5.5 \pm 2.1 \text{ cm}^{-3}$), that constituted a



potentially important additional source of total CCN not measured by the CCN system (0.14% SS: $44 \pm 25 \text{ cm}^{-3}$; 0.38% SS: $70 \pm 36 \text{ cm}^{-3}$), particularly at low supersaturations where they would be expected to activate first.

Deviations from this general picture arose when influxes of other aerosol types occurred. During the transit through an anthropogenic urban plume, size distributions were dominated by an Aitken mode with 80 to 90 nm median diameters that slowly transformed, with distance from the urban center, into a more typical mixed marine type population. After a marked increase in some VOC concentrations at 19Z on 17 Sept (3 AM local) a smaller ultrafine mode of particles was observed several hours later, possibly due to photochemical processes. Larger Aitken modal fractions with higher geometric standard deviations were observed, while the accumulation mode remained similar to the background marine type. A separate event marked by an increase in VOC measured by the gas canister samples occurred on 23 Sept, characterized by a different aerosol distribution that may have mixed from aloft.

In addition to these general classifications, several interesting periods during the 2012 cruise were observed that warrant additional discussion. Short lived intrusions (two to five hours) of accumulation mode particles were regularly observed in both the CCN system and PCASP datasets, and were classified as part of the mixed marine population type (e.g. 18-23Z on 22, 23, and 24 Sep) after which the size distributions quickly returned to clean marine conditions. These excursions were largely constrained to the pre-dawn hours (sunrise occurs around 22Z) when the boundary layer was thinnest, and when precipitation was occurring in the vicinity of the *Vasco*. Several prior studies have shown that smoke and anthropogenic pollution aerosol within the wider MC region can be lofted into and transported in the lower free troposphere (Tosca et al., 2011; Robinson et al., 2012; Zender et al., 2012; Campbell et al., 2013; Atwood et al., 2013). The influence of a free tropospheric aerosol layer as a source of MBL aerosol and CCN concentrations has been identified in other remote oceanic regions as well (Clarke et al., 2013). One possible explanation for these events, and possibly for the observed organic and ultrafine events that were characterized by increases in gas phase VOCs, is therefore that aerosol may have been mixed down into the MBL from a layer aloft, perhaps on the edge of rain shafts. However, they may also be due to intermittent plumes of aerosol that survived stochastic precipitation removal events along a boundary layer transport pathway or human terrestrial activities in the pre-dawn hours. Future work in the region may provide further insight into these events and the potential importance of an aerosol layer aloft.

5 Conclusion

This study reports ship based measurements of aerosol size distributions and CCN properties conducted as part of the first extensive, in situ aerosol measurement campaign in remote marine regions of the South China Sea/East Sea during the important Southwestern Monsoon and biomass burning season. Analysis of approximately two weeks of measurements found aerosol characteristics consistent with those from a previous pilot study in the region during the same season, indicating the regional and temporal representativeness of these results.



Eight aerosol population types were identified in the dataset. Many of the CCN-relevant differences between the aerosol population types (particularly for processes involving supersaturations at about 0.3% or higher) occurred in Aitken mode particles. It should be noted that many measurements of aerosol based on either optical or mass properties, including typical aerosol models and satellite retrievals, will be minimally impacted by Aitken mode particles, and therefore may not be especially sensitive to important changes in CCN abundance and properties as detected in with these in situ observations. Future work with this dataset will therefore investigate if coincident optical measurements of both dry and humidified aerosol can be related to CCN properties given the aerosol properties associated with population types found here.

Lastly, additional open questions remain regarding the relative importance of various sources and transport pathways of aerosol into remote MBL air masses. Since the surface-based observations provide only a portion of the observations needed to construct a true aerosol budget for the MBL, the degree to which MBL aerosol may be impacted by mixing down from a reservoir aloft was not clear. Future airborne aerosol campaigns in the region may be useful to shed light on this important topic.

Acknowledgments. Funding for this research cruise and analysis was provided from a number of sources. Vasco ship time procurement was provided by the NRL 6.1 Base Program via an ONR Global grant to the Manila Observatory. Core funding for this effort was from Office of Naval Research 322 under Award Number N00014-16-1-2040 and the Naval Research Enterprise Internship Program (NREIP). Funding for NRL scientist participation was provided by the NRL Base Program and ONR 35. This material is based upon research supported by the Office of Naval Research under Award Number N00014-16-1-2040, and by the Colorado State University Center for Geosciences/Atmospheric Research (CG/AR). We are most grateful to the Vasco ship management and crew, operated by Cosmix Underwater Research Ltd, (esp. Luc Heymans and Annabelle du Parc), the Manila Observatory senior management (esp. Antonia Loyzaga and Fr. Daniel McNamara), and the US State Department/ Embassy in Manila (esp. Maria Theresa Villa and Dovas Saulys).

References

Akagi, S. K., Yokelson, R. J., Wiedinmyer, C., Alvarado, M. J., Reid, J. S., Karl, T., Crouse, J. D. and Wennberg, P. O.: Emission factors for open and domestic biomass burning for use in atmospheric models, *Atmos Chem Phys*, 11(9), 4039–4072, doi:10.5194/acp-11-4039-2011, 2011.

Andreae, M. O. and Rosenfeld, D.: Aerosol–cloud–precipitation interactions. Part 1. The nature and sources of cloud-active aerosols, *Earth-Sci. Rev.*, 89(1–2), 13–41, doi:10.1016/j.earscirev.2008.03.001, 2008.

Andreae, M. O., Rosenfeld, D., Artaxo, P., Costa, A. A., Frank, G. P., Longo, K. M. and Silva-Dias, M. a. F.: Smoking Rain Clouds over the Amazon, *Science*, 303(5662), 1337–1342, doi:10.1126/science.1092779, 2004.

Atwood, S. A., Reid, J. S., Kreidenweis, S. M., Yu, L. E., Salinas, S. V., Chew, B. N. and Balasubramanian, R.: Analysis of source regions for smoke events in Singapore for the 2009 El Nino burning season, *Atmos. Environ.*, 78, 219–230, doi:10.1016/j.atmosenv.2013.04.047, 2013.



- Balasubramanian, R., Qian, W.-B., Decesari, S., Facchini, M. C. and Fuzzi, S.: Comprehensive characterization of PM_{2.5} aerosols in Singapore, *J. Geophys. Res. Atmospheres*, 108(D16), 4523, doi:10.1029/2002JD002517, 2003.
- Campbell, J. R., Reid, J. S., Westphal, D. L., Zhang, J., Tackett, J. L., Chew, B. N., Welton, E. J., Shimizu, A., Sugimoto, N., Aoki, K. and Winker, D. M.: Characterizing the vertical profile of aerosol particle extinction and linear depolarization over Southeast Asia and the Maritime Continent: The 2007–2009 view from CALIOP, *Atmospheric Res.*, 122, 520–543, doi:10.1016/j.atmosres.2012.05.007, 2013.
- Cavalli, F., Facchini, M. C., Decesari, S., Mircea, M., Emblico, L., Fuzzi, S., Ceburnis, D., Yoon, Y. J., O’Dowd, C. D., Putaud, J.-P. and Dell’Acqua, A.: Advances in characterization of size-resolved organic matter in marine aerosol over the North Atlantic, *J. Geophys. Res. Atmospheres*, 109(D24), D24215, doi:10.1029/2004JD005137, 2004.
- 10 Clarke, A. D., Owens, S. R. and Zhou, J.: An ultrafine sea-salt flux from breaking waves: Implications for cloud condensation nuclei in the remote marine atmosphere, *J. Geophys. Res. Atmospheres*, 111(D6), D06202, doi:10.1029/2005JD006565, 2006.
- Clarke, A. D., Freitag, S., Simpson, R. M. C., Hudson, J. G., Howell, S. G., Brekhovskikh, V. L., Campos, T., Kapustin, V. N. and Zhou, J.: Free troposphere as a major source of CCN for the equatorial pacific boundary layer: long-range transport and teleconnections, *Atmos Chem Phys*, 13(15), 7511–7529, doi:10.5194/acp-13-7511-2013, 2013.
- 15 Draxler, R. R. and Hess, G. D.: Description of the HYSPLIT4 modeling system, [online] Available from: <http://warn.arl.noaa.gov/documents/reports/arl-224.pdf> (Accessed 14 April 2015), 1997.
- Draxler, R. R. and Hess, G. D.: An overview of the HYSPLIT_4 modelling system for trajectories, *Aust. Meteorol. Mag.*, 47(4), 295–308, 1998.
- 20 Draxler, R. R., Stunder, B., Rolph, G. and Taylor, A.: HYSPLIT4 user’s guide, NOAA Tech. Memo. ERL ARL, 230, 35, 1999.
- Engelhart, G. J., Hennigan, C. J., Miracolo, M. A., Robinson, A. L. and Pandis, S. N.: Cloud condensation nuclei activity of fresh primary and aged biomass burning aerosol, *Atmos Chem Phys*, 12(15), 7285–7293, doi:10.5194/acp-12-7285-2012, 2012.
- 25 Facchini, M. C., Rinaldi, M., Decesari, S., Carbone, C., Finessi, E., Mircea, M., Fuzzi, S., Ceburnis, D., Flanagan, R., Nilsson, E. D., de Leeuw, G., Martino, M., Woeltjen, J. and O’Dowd, C. D.: Primary submicron marine aerosol dominated by insoluble organic colloids and aggregates, *Geophys. Res. Lett.*, 35(17), L17814, doi:10.1029/2008GL034210, 2008.
- Feingold, G., Cotton, W. R., Kreidenweis, S. M. and Davis, J. T.: The Impact of Giant Cloud Condensation Nuclei on Drizzle Formation in Stratocumulus: Implications for Cloud Radiative Properties, *J. Atmospheric Sci.*, 56(24), 4100–4117, doi:10.1175/1520-0469(1999)056<4100:TIOGCC>2.0.CO;2, 1999.
- 30 Feng, N. and Christopher, S. A.: Satellite and surface-based remote sensing of Southeast Asian aerosols and their radiative effects, *Atmospheric Res.*, 122, 544–554, doi:10.1016/j.atmosres.2012.02.018, 2013.
- Giglio, L., Descloitres, J., Justice, C. O. and Kaufman, Y. J.: An Enhanced Contextual Fire Detection Algorithm for MODIS, *Remote Sens. Environ.*, 87(2–3), 273–282, doi:10.1016/S0034-4257(03)00184-6, 2003.
- 35 Good, N., Topping, D. O., Allan, J. D., Flynn, M., Fuentes, E., Irwin, M., Williams, P. I., Coe, H. and McFiggans, G.: Consistency between parameterisations of aerosol hygroscopicity and CCN activity during the RHaMBLe discovery cruise, *Atmos Chem Phys*, 10(7), 3189–3203, doi:10.5194/acp-10-3189-2010, 2010.



- Hewitt, C. N., Lee, J. D., MacKenzie, A. R., Barkley, M. P., Carslaw, N., Carver, G. D., Chappell, N. A., Coe, H., Collier, C., Commane, R., Davies, F., Davison, B., DiCarlo, P., Di Marco, C. F., Dorsey, J. R., Edwards, P. M., Evans, M. J., Fowler, D., Furneaux, K. L., Gallagher, M., Guenther, A., Heard, D. E., Helfter, C., Hopkins, J., Ingham, T., Irwin, M., Jones, C., Karunaharan, A., Langford, B., Lewis, A. C., Lim, S. F., MacDonald, S. M., Mahajan, A. S., Malpass, S., McFiggans, G., Mills, G., Misztal, P., Moller, S., Monks, P. S., Nemitz, E., Nicolas-Perea, V., Oetjen, H., Oram, D. E., Palmer, P. I., Phillips, G. J., Pike, R., Plane, J. M. C., Pugh, T., Pyle, J. A., Reeves, C. E., Robinson, N. H., Stewart, D., Stone, D., Whalley, L. K. and Yin, X.: Overview: oxidant and particle photochemical processes above a south-east Asian tropical rainforest (the OP3 project): introduction, rationale, location characteristics and tools, *Atmos Chem Phys*, 10(1), 169–199, doi:10.5194/acp-10-169-2010, 2010.
- 5
- Hogan, T. F. and Rosmond, T. E.: The Description of the Navy Operational Global Atmospheric Prediction System's Spectral Forecast Model, *Mon. Weather Rev.*, 119(8), 1786–1815, doi:10.1175/1520-0493(1991)119<1786:TDOTNO>2.0.CO;2, 1991.
- 10
- Hoppel, W. A., Frick, G. M. and Larson, R. E.: Effect of nonprecipitating clouds on the aerosol size distribution in the marine boundary layer, *Geophys. Res. Lett.*, 13(2), 125–128, doi:10.1029/GL013i002p00125, 1986.
- Hoppel, W. A., Frick, G. M., Fitzgerald, J. W. and Larson, R. E.: Marine boundary layer measurements of new particle formation and the effects nonprecipitating clouds have on aerosol size distribution, *J. Geophys. Res. Atmospheres*, 99(D7), 14443–14459, doi:10.1029/94JD00797, 1994.
- 15
- Hussein, T., Dal Maso, M., Petäjä, T., Koponen, I. K., Paatero, P., Aalto, P. P., Hämeri, K. and Kulmala, M.: Evaluation of an automatic algorithm for fitting the particle number size distributions, *Boreal Environ. Res.*, 10(5), 337–355, 2005.
- Hyer, E. J., Reid, J. S., Prins, E. M., Hoffman, J. P., Schmidt, C. C., Miettinen, J. I. and Giglio, L.: Patterns of fire activity over Indonesia and Malaysia from polar and geostationary satellite observations, *Atmospheric Res.*, 122, 504–519, doi:10.1016/j.atmosres.2012.06.011, 2013.
- 20
- Irwin, M., Robinson, N., Allan, J. D., Coe, H. and McFiggans, G.: Size-resolved aerosol water uptake and cloud condensation nuclei measurements as measured above a Southeast Asian rainforest during OP3, *Atmos Chem Phys*, 11(21), 11157–11174, doi:10.5194/acp-11-11157-2011, 2011.
- 25
- Levin, E. J. T., McMeeking, G. R., Carrico, C. M., Mack, L. E., Kreidenweis, S. M., Wold, C. E., Moosmüller, H., Arnott, W. P., Hao, W. M., Collett, J. L. and Malm, W. C.: Biomass burning smoke aerosol properties measured during Fire Laboratory at Missoula Experiments (FLAME), *J. Geophys. Res. Atmospheres*, 115(D18), D18210, doi:10.1029/2009JD013601, 2010.
- 30
- Lin, N.-H., Sayer, A. M., Wang, S.-H., Loftus, A. M., Hsiao, T.-C., Sheu, G.-R., Hsu, N. C., Tsay, S.-C. and Chantara, S.: Interactions between biomass-burning aerosols and clouds over Southeast Asia: Current status, challenges, and perspectives, *Environ. Pollut.*, 195, 292–307, doi:10.1016/j.envpol.2014.06.036, 2014.
- Lynch, P., Reid, J. S., Westphal, D. L., Zhang, J., Hogan, T. F., Hyer, E. J., Curtis, C. A., Hegg, D. A., Shi, Y., Campbell, J. R., Rubin, J. I., Sessions, W. R., Turk, F. J. and Walker, A. L.: An 11-year global gridded aerosol optical thickness reanalysis (v1.0) for atmospheric and climate sciences, *Geosci Model Dev*, 9(4), 1489–1522, doi:10.5194/gmd-9-1489-2016, 2016.
- 35
- O'Dowd, C. D. and Leeuw, G. de: Marine aerosol production: a review of the current knowledge, *Philos. Trans. R. Soc. Math. Phys. Eng. Sci.*, 365(1856), 1753–1774, doi:10.1098/rsta.2007.2043, 2007.



- O'Dowd, C. D., Smith, M. H., Consterdine, I. E. and Lowe, J. A.: Marine aerosol, sea-salt, and the marine sulphur cycle: a short review, *Atmos. Environ.*, 31(1), 73–80, doi:10.1016/S1352-2310(96)00106-9, 1997.
- O'Dowd, C. D., Facchini, M. C., Cavalli, F., Ceburnis, D., Mircea, M., Decesari, S., Fuzzi, S., Yoon, Y. J. and Putaud, J.-P.: Biogenically driven organic contribution to marine aerosol, *Nature*, 431(7009), 676–680, doi:10.1038/nature02959, 2004.
- 5 Pedregosa, F., Varoquaux, G., Gramfort, A., Michel, V., Thirion, B., Grisel, O., Blondel, M., Prettenhofer, P., Weiss, R., Dubourg, V., Vanderplas, J., Passos, A., Cournapeau, D., Brucher, M., Perrot, M. and Duchesnay, É.: Scikit-learn: Machine Learning in Python, *J Mach Learn Res*, 12, 2825–2830, 2011.
- Petters, M. D. and Kreidenweis, S. M.: A single parameter representation of hygroscopic growth and cloud condensation nucleus activity, *Atmos Chem Phys*, 7(8), 1961–1971, doi:10.5194/acp-7-1961-2007, 2007.
- 10 Petters, M. D., Carrico, C. M., Kreidenweis, S. M., Prenni, A. J., DeMott, P. J., Collett, J. L. and Moosmüller, H.: Cloud condensation nucleation activity of biomass burning aerosol, *J. Geophys. Res. Atmospheres*, 114(D22), D22205, doi:10.1029/2009JD012353, 2009.
- Prather, K. A., Bertram, T. H., Grassian, V. H., Deane, G. B., Stokes, M. D., DeMott, P. J., Aluwihare, L. I., Palenik, B. P., Azam, F., Seinfeld, J. H., Moffet, R. C., Molina, M. J., Cappa, C. D., Geiger, F. M., Roberts, G. C., Russell, L. M., Ault, A. P., Baltrusaitis, J., Collins, D. B., Corrigan, C. E., Cuadra-Rodriguez, L. A., Ebben, C. J., Forestieri, S. D., Guasco, T. L., Hersey, S. P., Kim, M. J., Lambert, W. F., Modini, R. L., Mui, W., Pedler, B. E., Ruppel, M. J., Ryder, O. S., Schoepp, N. G., Sullivan, R. C. and Zhao, D.: Bringing the ocean into the laboratory to probe the chemical complexity of sea spray aerosol, *Proc. Natl. Acad. Sci.*, 110(19), 7550–7555, doi:10.1073/pnas.1300262110, 2013.
- 20 Reid, J. S., Hyer, E. J., Prins, E. M., Westphal, D. L., Zhang, J., Wang, J., Christopher, S. A., Curtis, C. A., Schmidt, C. C., Eleuterio, D. P., Richardson, K. A. and Hoffman, J. P.: Global Monitoring and Forecasting of Biomass-Burning Smoke: Description of and Lessons From the Fire Locating and Modeling of Burning Emissions (FLAMBE) Program, *IEEE J. Sel. Top. Appl. Earth Obs. Remote Sens.*, 2(3), 144–162, doi:10.1109/JSTARS.2009.2027443, 2009.
- 25 Reid, J. S., Xian, P., Hyer, E. J., Flatau, M. K., Ramirez, E. M., Turk, F. J., Sampson, C. R., Zhang, C., Fukada, E. M. and Maloney, E. D.: Multi-scale meteorological conceptual analysis of observed active fire hotspot activity and smoke optical depth in the Maritime Continent, *Atmos Chem Phys*, 12(4), 2117–2147, doi:10.5194/acp-12-2117-2012, 2012.
- 30 Reid, J. S., Hyer, E. J., Johnson, R. S., Holben, B. N., Yokelson, R. J., Zhang, J., Campbell, J. R., Christopher, S. A., Di Girolamo, L., Giglio, L., Holz, R. E., Kearney, C., Miettinen, J., Reid, E. A., Turk, F. J., Wang, J., Xian, P., Zhao, G., Balasubramanian, R., Chew, B. N., Janjai, S., Lagrosas, N., Lestari, P., Lin, N.-H., Mahmud, M., Nguyen, A. X., Norris, B., Oanh, N. T. K., Oo, M., Salinas, S. V., Welton, E. J. and Liew, S. C.: Observing and understanding the Southeast Asian aerosol system by remote sensing: An initial review and analysis for the Seven Southeast Asian Studies (7SEAS) program, *Atmospheric Res.*, 122, 403–468, doi:10.1016/j.atmosres.2012.06.005, 2013.
- 35 Reid, J. S., Lagrosas, N. D., Jonsson, H. H., Reid, E. A., Sessions, W. R., Simpas, J. B., Uy, S. N., Boyd, T. J., Atwood, S. A., Blake, D. R., Campbell, J. R., Cliff, S. S., Holben, B. N., Holz, R. E., Hyer, E. J., Lynch, P., Meinardi, S., Posselt, D. J., Richardson, K. A., Salinas, S. V., Smirnov, A., Wang, Q., Yu, L. and Zhang, J.: Observations of the temporal variability in aerosol properties and their relationships to meteorology in the summer monsoonal South China Sea/East Sea: the scale-dependent role of monsoonal flows, the Madden–Julian Oscillation, tropical cyclones, squall lines and cold pools, *Atmos Chem Phys*, 15(4), 1745–1768, doi:10.5194/acp-15-1745-2015, 2015.
- 40 Reid, J. S., Lagrosas, N. D., Jonsson, H. H., Reid, E. A., Atwood, S. A., Boyd, T. J., Ghate, V. P., Lynch, P., Posselt, D. J., Simpas, J. B., Uy, S. N., Zaiger, K., Blake, D. R., Bucholtz, A., Campbell, J. R., Chew, B. N., Cliff, S. S., Holben, B. N., Holz, R. E., Hyer, E. J., Kreidenweis, S. M., Kuciaskas, A. P., Lolli, S., Oo, M., Perry, K. D., Salinas, S. V., Sessions, W. R.,



- Smirnov, A., Walker, A. L., Wang, Q., Yu, L., Zhang, J. and Zhao, Y.: Aerosol meteorology and Philippine receptor observations of Maritime Continent aerosol emissions for the 2012 7SEAS southwest monsoon intensive study, *Atmospheric Chem. Phys. Discuss.*, 1–61, doi:10.5194/acp-2016-214, 2016.
- 5 Robinson, N. H., Newton, H. M., Allan, J. D., Irwin, M., Hamilton, J. F., Flynn, M., Bower, K. N., Williams, P. I., Mills, G., Reeves, C. E., McFiggans, G. and Coe, H.: Source attribution of Bornean air masses by back trajectory analysis during the OP3 project, *Atmos Chem Phys*, 11(18), 9605–9630, doi:10.5194/acp-11-9605-2011, 2011.
- Robinson, N. H., Allan, J. D., Trembath, J. A., Rosenberg, P. D., Allen, G. and Coe, H.: The lofting of Western Pacific regional aerosol by island thermodynamics as observed around Borneo, *Atmos Chem Phys*, 12(13), 5963–5983, doi:10.5194/acp-12-5963-2012, 2012.
- 10 Rose, D., Nowak, A., Achtert, P., Wiedensohler, A., Hu, M., Shao, M., Zhang, Y., Andreae, M. O. and Pöschl, U.: Cloud condensation nuclei in polluted air and biomass burning smoke near the mega-city Guangzhou, China – Part 1: Size-resolved measurements and implications for the modeling of aerosol particle hygroscopicity and CCN activity, *Atmos Chem Phys*, 10(7), 3365–3383, doi:10.5194/acp-10-3365-2010, 2010.
- Rosenfeld, D.: TRMM observed first direct evidence of smoke from forest fires inhibiting rainfall, *Geophys. Res. Lett.*, 15 26(20), 3105–3108, doi:10.1029/1999GL006066, 1999.
- Shank, L. M., Howell, S., Clarke, A. D., Freitag, S., Brekhovskikh, V., Kapustin, V., McNaughton, C., Campos, T. and Wood, R.: Organic matter and non-refractory aerosol over the remote Southeast Pacific: oceanic and combustion sources, *Atmos Chem Phys*, 12(1), 557–576, doi:10.5194/acp-12-557-2012, 2012.
- 20 Spracklen, D. V., Pringle, K. J., Carslaw, K. S., Mann, G. W., Manktelow, P. and Heintzenberg, J.: Evaluation of a global aerosol microphysics model against size-resolved particle statistics in the marine atmosphere, *Atmos Chem Phys*, 7(8), 2073–2090, doi:10.5194/acp-7-2073-2007, 2007.
- Tosca, M. G., Randerson, J. T., Zender, C. S., Nelson, D. L., Diner, D. J. and Logan, J. A.: Dynamics of fire plumes and smoke clouds associated with peat and deforestation fires in Indonesia, *J. Geophys. Res. Atmospheres*, 116(D8), D08207, doi:10.1029/2010JD015148, 2011.
- 25 Wang, J., Ge, C., Yang, Z., Hyer, E. J., Reid, J. S., Chew, B.-N., Mahmud, M., Zhang, Y. and Zhang, M.: Mesoscale modeling of smoke transport over the Southeast Asian Maritime Continent: Interplay of sea breeze, trade wind, typhoon, and topography, *Atmospheric Res.*, 122, 486–503, doi:10.1016/j.atmosres.2012.05.009, 2013.
- Wilks, D. S.: *Statistical Methods in the Atmospheric Sciences*, Academic Press., 2011.
- Xian, P., Reid, J. S., Atwood, S. A., Johnson, R. S., Hyer, E. J., Westphal, D. L. and Sessions, W.: Smoke aerosol transport patterns over the Maritime Continent, *Atmospheric Res.*, 122, 469–485, doi:10.1016/j.atmosres.2012.05.006, 2013.
- 30 Yokelson, R. J., Christian, T. J., Karl, T. G. and Guenther, A.: The tropical forest and fire emissions experiment: laboratory fire measurements and synthesis of campaign data, *Atmos Chem Phys*, 8(13), 3509–3527, doi:10.5194/acp-8-3509-2008, 2008.
- Yuan, T., Remer, L. A., Pickering, K. E. and Yu, H.: Observational evidence of aerosol enhancement of lightning activity and convective invigoration, *Geophys. Res. Lett.*, 38(4), L04701, doi:10.1029/2010GL046052, 2011.



Zender, C. S., Krolewski, A. G., Tosca, M. G. and Randerson, J. T.: Tropical biomass burning smoke plume size, shape, reflectance, and age based on 2001–2009 MISR imagery of Borneo, Atmos Chem Phys, 12(7), 3437–3454, doi:10.5194/acp-12-3437-2012, 2012.

5

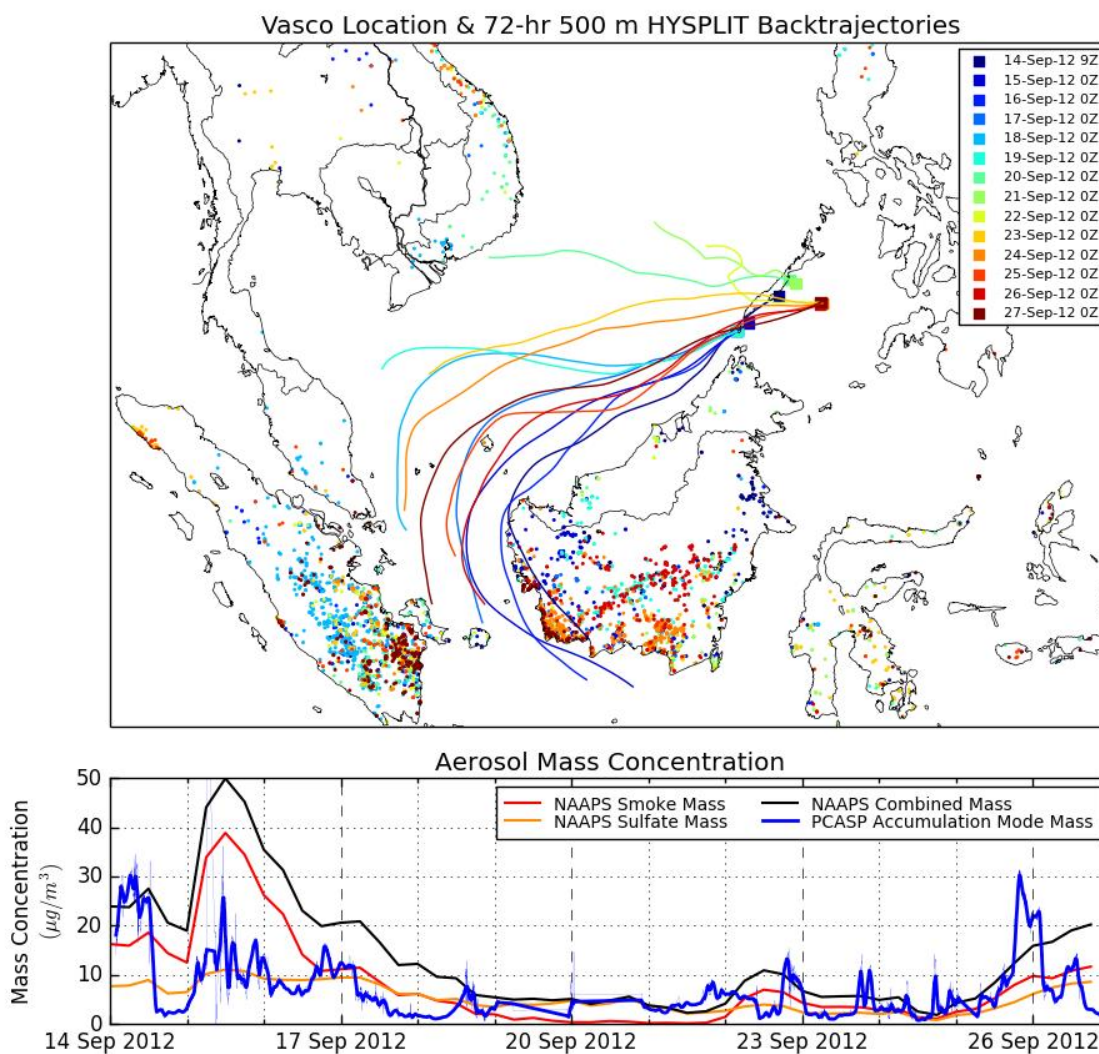


Figure 1: (a) *Vasco* cruise locations (squares) and 72-hour, 500 m HYSPLIT backtrajectories; MODIS fire detections (dots) from Terra and Aqua are included for each day (color coded) during the sampling period. (b) PCASP reconstructed accumulation mode (125nm – 800nm) mass concentration (assumed density $1.4 \mu\text{g m}^{-3}$) and NAAPS estimated smoke and sulfate mass concentration along the *Vasco* ship-track.

10

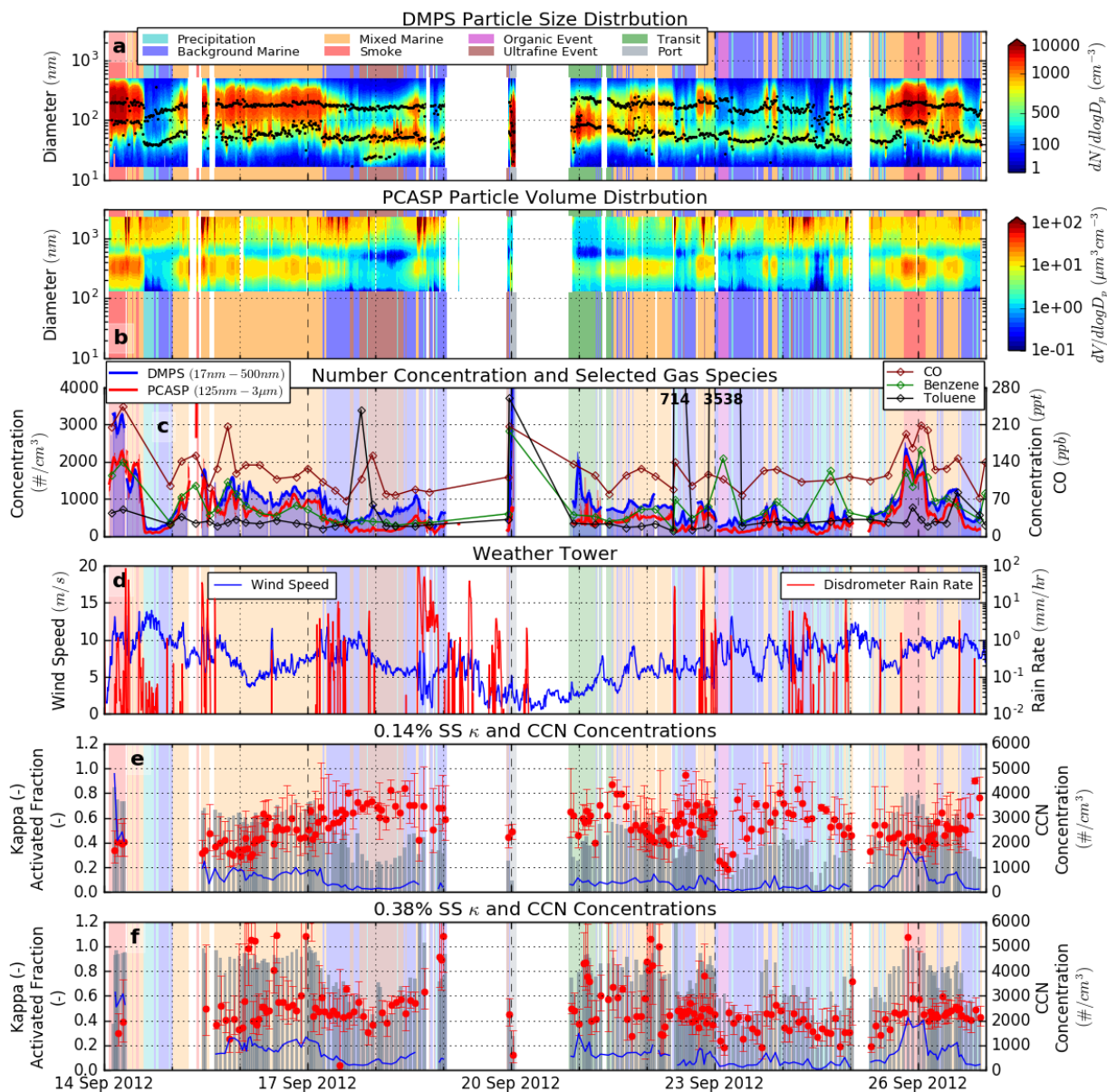


Figure 2: Timelines of measured and derived variables during *Vasco* 2012 cruise. In all figures, background colors correspond to aerosol type classification from the cluster analysis, as indicated in the legend in panel a. (a) $dN/d\log D_p$ spectra from the CCN system measurements with black dots at best-fit modal median diameters; (b) $dV/d\log D_p$ spectra derived from the PCASP measurements; (c) total number concentrations measured by the CCN system (blue; shaded below for contrast) and the PCASP measurements; (d) total number concentrations measured by the CCN system (blue; shaded below for contrast) and the PCASP measurements, with 60 minute boxcar average smoothing; gas canister grab sample concentrations for carbon monoxide, benzene, and toluene are shown on the right axis with colored numbers indicating sample points above the upper scale extent; (e) wind speed and disdrometer rain rate from the *Vasco* weather tower. (e & f) κ parameter (red) and CCN concentrations (blue) for 0.14% and 0.38% supersaturation settings (corresponding approximately to accumulation and Aitken modes, respectively), with total activated particle number fractions ($CCN_{SS\%} / CN_{Total}$) bars in grey. Error bars on κ data points indicate the κ values associated with 25% / 75% activated fraction curve fits.

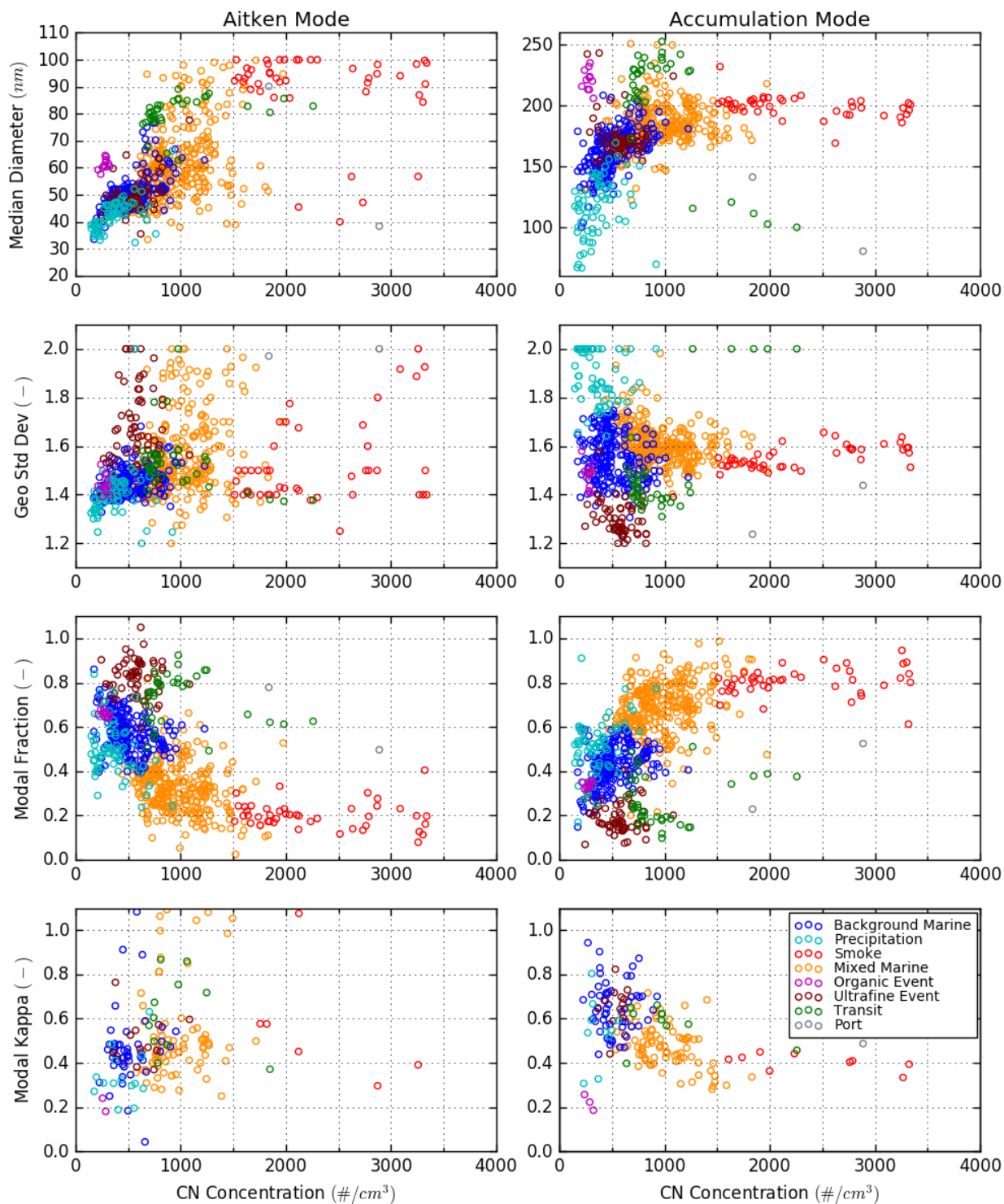




Figure 3: Parameterized variable values for Aitken and accumulation modes (median diameter, geometric standard deviation, modal fraction) at each of the 15 minute data points during the study, along with κ values for data points at CCNc superstation set points of 0.38% (Aitken mode) and 0.14% (accumulation mode). Each data point is colored according to the cluster type to which it was classified.



Normalized $d\bar{N}/d\log D_p$

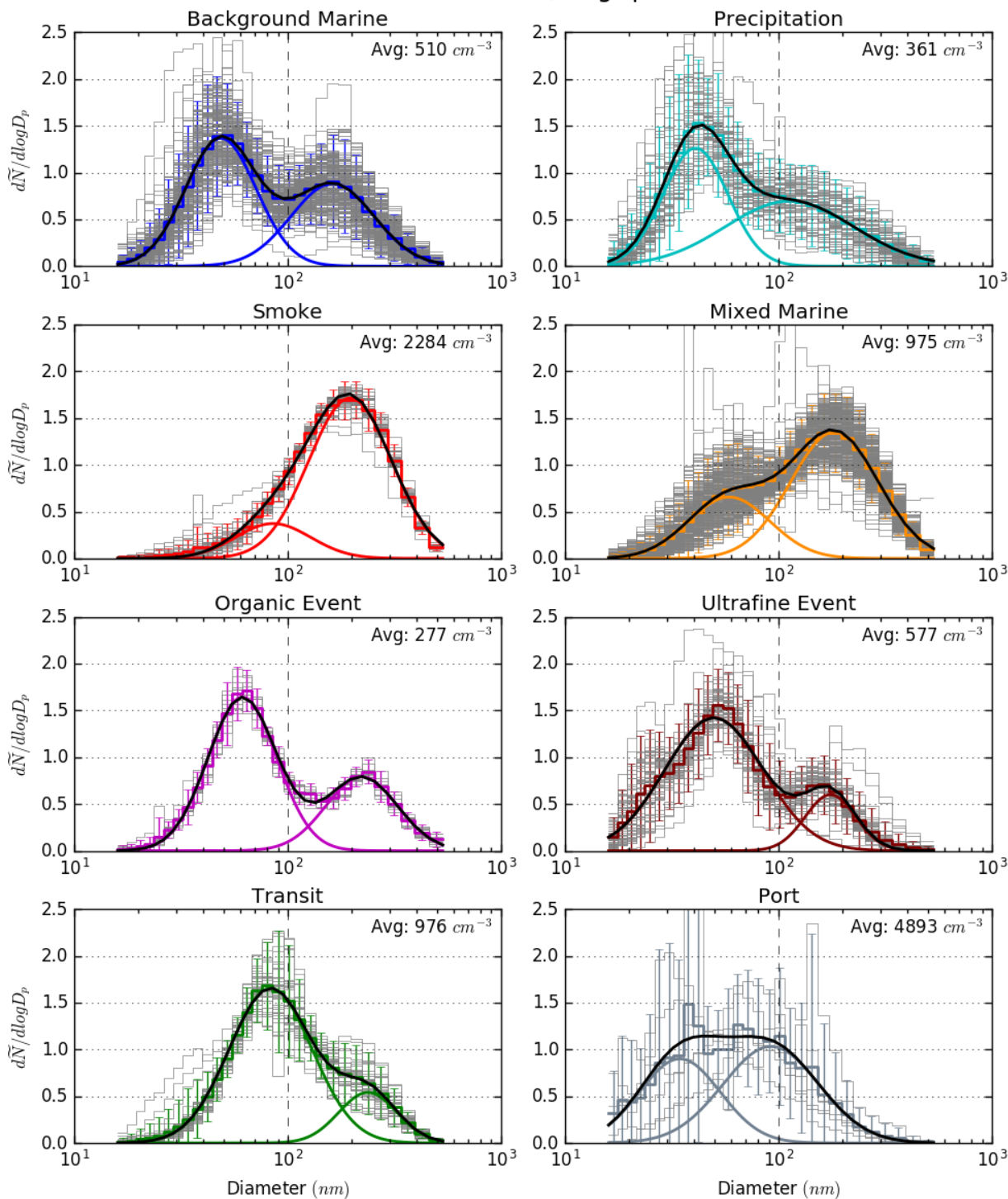
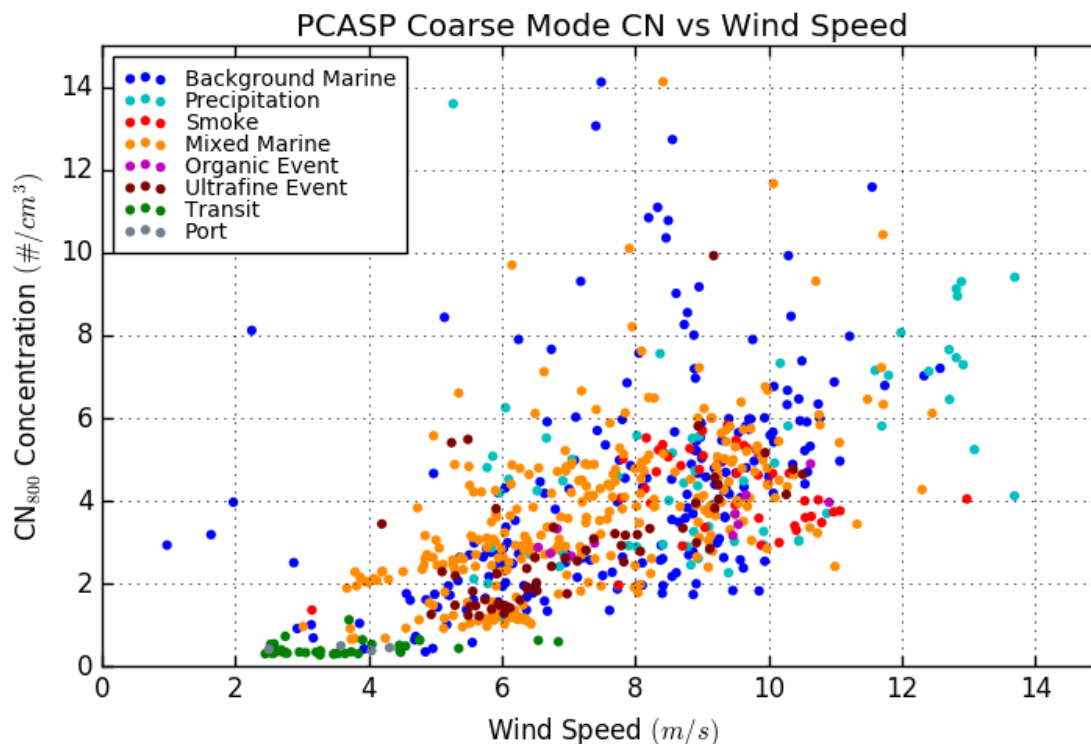




Figure 4: Normalized $dN/d\log D_p$ particle size distributions for each spectra within identified aerosol population types (grey), the associated average bin values with error bars at 95% confidence interval (colored step lines; $1.96 * \text{bin standard deviation}$), and best fit lognormal modes (colored curves) with bimodal fit (black). The average particle number concentrations of data points within each population type are listed.



5

Figure 5: Number concentrations of coarse mode particles ($D_p > 800 \text{ nm}$) measured by the PCASP as functions of local surface wind speed measured by the onboard *Vasco* weather station. Each point was averaged over the same approximately 15 minute time period as for the CCN system measurements, and is colored by the aerosol type as described in the text.



Table 1: Average values (standard deviations in grey parentheses) for identified aerosol population types. Shown are number of CCN system data points classified as each type, total number concentrations for the PCASP (125 nm–3 μm) and CCN system (17–500 nm), CCN number concentrations and activated fractions for each CCNc supersaturation set point, and measured κ values for the accumulation mode (0.14% SS) and Aitken mode (0.38% SS) set points.

Population Type	# CCN Meas. (#)	PCASP Number (#/cm ³)	CCN system Number (#/cm ³)	0.14% SS		0.38% SS		0.53% SS		0.71% SS		0.85% SS			
				CCN (#/cm ³)	Act Frac (-)	κ (-)	CCN (#/cm ³)	Act Frac (-)	κ (-)	CCN (#/cm ³)	Act Frac (-)	CCN (#/cm ³)	Act Frac (-)	CCN (#/cm ³)	Act Frac (-)
1: Back. Marine	214	231 (111)	510 (181)	213 (101)	0.38 (0.09)	0.65 (0.11)	320 (148)	0.60 (0.12)	0.46 (0.17)	416 (194)	0.74 (0.11)	444 (239)	0.81 (0.09)	480 (210)	0.87 (0.05)
2: Precipitation	67	142 (79)	361 (164)	96 (58)	0.24 (0.11)	0.54 (0.14)	243 (135)	0.48 (0.15)	0.34 (0.11)	352 (175)	0.65 (0.15)	265 (82)	0.71 (0.09)	228 (100)	0.79 (0.03)
3: Smoke	44	1800 (273)	2280 (606)	1720 (388)	0.72 (0.04)	0.40 (0.03)	2340 (480)	0.93 (0.02)	0.56 (0.25)	1990 (359)	0.97 (0.02)	2080 (396)	0.98 (0.05)	2150 (523)	0.99 (0.02)
4: Mixed Marine	294	689 (295)	975 (271)	591 (201)	0.58 (0.08)	0.48 (0.10)	827 (270)	0.83 (0.07)	0.54 (0.23)	861 (247)	0.89 (0.10)	876 (244)	0.94 (0.06)	893 (271)	0.96 (0.05)
5: Organic Event	11	151 (19)	277 (30)	88 (10)	0.31 (0.02)	0.22 (0.03)	144 (9)	0.53 (0.01)	0.21 (0.03)	182 (26)	0.72 (0.01)	268 (56)	0.89 (0.14)	257 (24)	0.93 (0.07)
6: Ultrafine Event	59	163 (58)	577 (158)	138 (45)	0.25 (0.06)	0.65 (0.09)	361 (172)	0.56 (0.11)	0.50 (0.10)	373 (168)	0.65 (0.12)	439 (163)	0.72 (0.07)	473 (147)	0.79 (0.10)
7: Transit	36	311 (44)	976 (384)	363 (87)	0.37 (0.06)	0.58 (0.08)	772 (263)	0.81 (0.09)	0.62 (0.16)	832 (423)	0.87 (0.05)	877 (370)	0.90 (0.02)	878 (195)	0.95 (0.03)
8: Port	6	671 (210)	4890 (2550)	251 (-)*	0.09 (-)*	0.49 (-)*	1126 (-)*	0.26 (-)*	0.13 (-)*	3936 (-)*	0.40 (-)*	1742 (289)	0.57 (0.22)	2080 (-)*	0.45 (-)*
All Types	731	503 (455)	851 (677)	450 (388)	0.47 (0.16)	0.54 (0.14)	675 (516)	0.72 (0.17)	0.50 (0.21)	698 (555)	0.79 (0.15)	724 (512)	0.85 (0.13)	723 (502)	0.90 (0.10)

5 * Only one datapoint; Note that Port measurements fluctuated as the Vasco entered port